2022 IEEE 11th Data Driven Control and Learning Systems Conference
August 5-7, 2022, Emeishan, China

Discrete-Time Integral Terminal Sliding Mode based Repetitive Control for Periodic Motion Tracking

Zhao Feng[1], Jie Ling[2], Yayi Shen[2]

1. Department of Electrical and Computer Engineering, University of Macau, Macao, P. R. China
E-mail: zhaofeng@um.edu.mo

2. College of Mechanical & Electrical Engineering, Nanjing University of Aeronautics and Astronautics, Nanjing 210016, P. R. China
E-mail: meejling@nuaa.edu.cn;yayi.shen@nuaa.edu.cn

Abstract:
The high precision position tracking in many industrial and scientific devices is vital for various tasks. Among these, periodic signals are commonly used in the condition that the references are given or planned in advance. In this paper, a discrete-time integral terminal sliding mode based repetitive control (DTITSMRC) is developed for periodic motion tracking. The discrete-time integral terminal sliding surface is employed for a fast convergence, and the repetitive control law with this sliding surface is integrated into the control scheme to further improve the performance through learning the information of the previous period. The quasi sliding mode band (QSMB) constrained for any initial state and the finite-time steps to QSMB with DTITSMRC are proven respectively. The simulation results on a discrete-time system demonstrate the effectiveness on periodic motion tracking for various signals.

Key Words: Periodic Motion Tracking, Discrete-Time Repetitive Control, Sliding Mode Control,

2022 IEEE 11th Data Driven Control and Learning Systems Conference (DDCLS) | 978-1-6654-9675-9/22/$31.00 ©2022 IEEE | DOI: 10.1109/DDCLS55054.2022.9858381

1 Introduction

Many industrial and scientific devices require precision position tracking to complete the anticipated tasks. Typically, the high-speed and precision tracking of linear motors is vital for the computer numerical control (CNC) micro machining [1, 2]; and the tracking precision of the piezoelectric nanopositioning stage mostly determines the imaging quality of the samples in a scanning probe microscope (SPM) [3–5]. To achieve the desired objective, various control methods could provide effective solutions for performance improvements.

Sliding mode control (SMC) is a nonlinear control method to achieve the robustness to parameter uncertainties and disturbance by enforcing the error states to the sliding surface, and then maintaining it around by the switching term [6, 7]. The linear sliding surface with linear operations on the states is widely used but with infinite-time convergence to zero errors [8]. To improve the convergence speed, the terminal SMC with fractional-order term in the sliding surface is developed to achieve the finite-time stability [9, 10]. In general, SMC can be designed based on the continuous-time domain resulting in that the high-order states of the system should be measured or estimated through extra sensors or delicately designed observers, especially for the high-order SMC [11]. However, the actual implementation of controller is generally realized on the digital control system. Thus, it is natural to design the controller on the discrete-time domain. In [12], a second-order discrete-time terminal SMC was proposed for the piezoelectric nanopositioning stage, and further a chattering-free discrete-time SMC was developed in [13]. It should be pointed out that the above methods could track any trajectory but without considering the property of the references.

This work is supported by the National Science Foundation of Jiangsu Province of China [Grant No.: BK20210294], and in part by the University of Macau under UM Macao Talent Programme [Grant No.:UMMTP-2020-01].

In many applications, the reference signals are given or planned in advance. With the knowledge of references, learning based control could further improve the performance. Iterative learning control (ILC) concentrates on the repetitive process in iteration domain, which requires the same initial condition of the reference, and takes several trials to converge to the desired performance [14]. Alternatively, periodic trajectories are also commonly tracked such as the scanning motion of SPM, where some signals are sinusoidal waves or triangular waves [4]. Thus, repetitive control (RC) utilizing the information of references' period is perfect for such motion patterns. In general, RCs are implemented by the parallel form with well-designed L-filter, Q-filter [3, 15]. Although continuous-time RC was proposed in [16] for nanopositioning, the discrete-time RC is more widely used and suitable for implementing on digital control systems. However, according to the internal model principle, the non-periodic errors will be amplified by the RC, indicating that the traditional RCs are lack of robustness to the non-periodic uncertainties so that the tracking performance could be deteriorated significantly under such conditions.

Motivated by above-mentioned discussions, a discrete-time integral terminal sliding mode based repetitive control (DTITSMRC) is proposed dedicating to the precision tracking of periodic motion. In this control scheme, a discrete-time integral terminal sliding function is utilized to achieve better steady-state performance and faster convergence. Then, the RC is combined into the method by virtual of the information of previous period. The quasi sliding mode band (QSMB) constrained for any initial state and the finite-time steps to QSMB with proposed DTITSMRC are proven respectively. Finally, the simulation cases for periodic signals' tracking are conducted to verify the effectiveness of the proposed controller. Through integrating the robustness to unexpected disturbances of SMC with the learning ability of RC for periodic signals, the proposed DTITSMRC takes both the advantages of SMC and RC. Moreover, only the input and output data are employed to

978-1-6654-9675-9/22/$31.00 ©2022 IEEE

implement the proposed controller without the need of extra sensors or state observers.

2 Preliminaries

Considering a discrete-time single input single output (SISO) system, the input-output equation is given as

$$y_k = \sum_{i=1}^{n} a_i y_{k-i} + \sum_{i=1}^{m} b_i u_{k-i} + p_k, \tag{1}$$

where $y_k \in \mathbb{R}$, $u_k \in \mathbb{R}$, and $p_k \in \mathbb{R}$ are the measured output, control force, and external disturbance, respectively. The symbol $k \in \mathbb{N}_+$ is denoted as the sampling point. $a_i \in \mathbb{R}$ and $b_i \in \mathbb{R}$ are the identified and known parameters of the plant, and n, m are positive integers with $n \geq m$.

In order to facilitate the controller design, the state-space representation of (1) can be described as

$$\begin{cases} X_{k+1} = AX_k + Bu_k + WQ_k + P_k \\ y_k = CX_k \end{cases}, \tag{2}$$

where

$$A = \begin{bmatrix} 0 & 1 & \cdots & 0 \\ \vdots & \vdots & \ddots & \vdots \\ 0 & 0 & \cdots & 1 \\ -a_n & -a_{n-1} & \cdots & -a_1 \end{bmatrix} \in \mathbb{R}^{n\times n},$$

$$B = \begin{bmatrix} 0 & \cdots & 0 & b_1 \end{bmatrix}^\top \in \mathbb{R}^{n\times 1}, \tag{3}$$

$$W = \begin{bmatrix} 0 & 0 & \cdots & 0 \\ \vdots & \vdots & \ddots & \vdots \\ 0 & 0 & \cdots & 0 \\ b_m & b_{m-1} & \cdots & b_2 \end{bmatrix} \in \mathbb{R}^{n\times(m-1)},$$

$$C = \begin{bmatrix} 0 & \cdots & 0 & 1 \end{bmatrix} \in \mathbb{R}^{1\times n},$$

$$X_k = \begin{bmatrix} x_{k-n+1} & \cdots & x_{k-1} & x_k \end{bmatrix}^\top \in \mathbb{R}^{n\times 1},$$

$$Q_k = \begin{bmatrix} u_{k-m+1} & \cdots & u_{k-2} & u_{k-1} \end{bmatrix}^\top \in \mathbb{R}^{(m-1)\times 1},$$

$$P_k = \begin{bmatrix} 0 & \cdots & 0 & p_k \end{bmatrix}^\top \in \mathbb{R}^{n\times 1}.$$

It can be observed from the above equations that the output y_k is equal to the last term of the state variables X_k so that the (4) can be calculated by the measured historical output data [12]. Therefore, no state observer is needed when implementing the proposed controller. Furthermore, $r_k \in \mathbb{R}_+$ is periodic in this paper. Therefore, we have

$$r_k = r_{k-N}, \tag{4}$$

where $N \in \mathbb{N}_+$ is the number of sample points per period of the signal of a digital control system.

With the dynamics (2), the objective of this paper is to track the desired periodic trajectory r_k at the presence of complex and unknown disturbance p_k.

3 Discrete-Time Integral Terminal Sliding Mode based Repetitive Controller Design

3.1 Definition of Sliding Mode Function

SMC is an effective methodology to improve the robustness of a plant suffering from external disturbance so that the performance could be improved [17]. The tracking error is defined as

$$e_k = y_k - r_k. \tag{5}$$

Here, a discrete-time integral terminal sliding function is used to drive e_k onto a specified sliding surface, defined as

$$s_k = c_1 e_k + c_2 E_{k-1}, \tag{6}$$

and the integral term is given by

$$E_k = \sum_{i=0}^{k} \text{sig}^\alpha e_k = E_{k-1} + \text{sig}^\alpha e_k, \tag{7}$$

where $c_1 > 0, c_2 > 0$, and $0 < \alpha < 1$, $\text{sig}^\alpha(e_k) = \text{sgn}(e_k) \cdot |e_k|^\alpha$. It should be noted that the fractional order α of e_k makes a faster convergence rate in comparison with a conventional linear sliding mode function [18]. Furthermore, the usage of the term $\text{sig}(\cdot)$ avoids the singular values when $e_k < 0$.

3.2 Design of DTITSMRC Scheme

Based on the sliding mode function, the followings give the definitions of quasi sliding mode (QSM) and its reaching condition, which are helpful for the controller design.

Definition 1(see [19, 20]). For a discrete-time plant, the system is said to achieve the QSM for any $\forall k \geq k^*$ if the sliding mode function satisfies

$$|s(k)| < \Delta, \tag{8}$$

where Δ is the width where the QSM happens, i.e., QSM band (QSMB).

Definition 2 (see [18, 21]). The reaching condition to QSM in the vicinity Δ of the sliding mode function if the following conditions hold:

$$\begin{aligned} &s_k > \Delta \rightarrow -\Delta \leq s(k+1) < s_k, \\ &s_k < -\Delta \rightarrow s_k < s_{k+1} \leq \Delta, \\ &|s_k| \leq \Delta \rightarrow |s_{k+1}| \leq \Delta. \end{aligned} \tag{9}$$

Furthermore, it is natural that the disturbance is bounded [22, 23]. Hence, the following assumption is employed.

Assumption 1. The disturbance term p_k can be decomposed as

$$p_k = p_{k-N} + \overline{p}_k, \tag{10}$$

and the increment disturbance $\overline{p}_k$ is bounded by $|\overline{p}_k| < \delta$, where δ is a positive constant.

Theorem 1. For the discrete-time system (2) with the periodic reference r_k, if the proposed DTITSMRC law is given as

$$\begin{aligned} u_k =& u_{k-N} + (c_1 CB)^{-1}[(1-\rho)s_k - \varepsilon \text{sgn}(s_k) - c_2 E_k - \\ & c_1 CA(X_k - X_{k-N}) + c_1 CWQ_{k-N} - \\ & s_{k+1-N} + c_2 E_{k-N}], \end{aligned} \tag{11}$$

where $0 < \rho < 1$, and the switching gain c_1 satisfies

$$\frac{\varepsilon}{c_1} > \delta > 0, \tag{12}$$

the sliding function will be constrained by the QSMB for any initial states, which is given as

$$\Delta = \frac{\varepsilon - c_1\delta}{2-\rho}. \tag{13}$$

Proof of Theorem 1. According to the sliding mode function (6), s_{k+1} can be expressed as

$$s_{k+1} = c_1 e_{k+1} + c_2 E_k. \tag{14}$$

With $e_{k+1} = y_{k+1} - r_{k+1}$, it is obtained that

$$s_{k+1} = c_1(y_{k+1} - r_{k+1}) + c_2 E_k. \tag{15}$$

Combining with the state-space representation (1), we have

$$\begin{aligned} s_{k+1} =& c_1 C X_{k+1} - c_1 r_{k+1} + c_2 E_k \\ =& c_1 C(AX_k + Bu_k + WQ_k + P_k) - c_1 r_{k+1} \\ &+ c_2 E_k. \end{aligned} \tag{16}$$

Substituting the control law (11) into (16), it is derived that

$$\begin{aligned} s_{k+1} =& c_1 C(AX_{k-N} + Bu_{k-N} + WQ_{k-N} + P_k) - c_1 \\ & r_{k+1-N} + c_2 E_{k-N} - s_{k+1-N} + (1-\rho)s_k - \\ & \varepsilon \mathrm{sgn}(s_k) \\ =& c_1 C X_{k+1-N} - c_1 r_{k+1-N} + c_2 E_{k-N} - s_{k+1-N} + \\ & (1-\rho)s_k - \varepsilon \mathrm{sgn}(s_k) + c_1 C \overline{P}_k \\ =& c_1(y_{k+1-N} - r_{k+1-N}) + c_2 E_{k-N} - s_{k+1-N} + \\ & (1-\rho)s_k - \varepsilon \mathrm{sgn}(s_k) + c_1 C \overline{P}_k \\ =& s_{k+1-N} - s_{k+1-N} + (1-\rho)s_k - \varepsilon \mathrm{sgn}(s_k) + c_1 \overline{p}_k \\ =& (1-\rho)s_k - \varepsilon \mathrm{sgn}(s_k) + c_1 \overline{p}_k, \end{aligned} \tag{17}$$

For s_k outside the QSMB, the reaching condition [24] is equivalent to

$$\begin{cases} (s_{k+1} - s_k)\mathrm{sgn}(s_k) < 0 \\ (s_{k+1} + s_k)\mathrm{sgn}(s_k) > 0 \end{cases}. \tag{18}$$

In the following, two cases are considered, i.e., the positive and negative values of s_k.

Case 1: If $s_k > 0$, according to (17) and (18), we have

$$\begin{cases} -\rho s_k - \varepsilon + c_1\overline{p}_k < 0 \\ (2-\rho)s_k - \varepsilon + c_1\overline{p}_k > 0 \end{cases}. \tag{19}$$

Combining with the bounded $|\overline{p}_k| < \delta$, it is derived that

$$\begin{cases} -\rho s_k - \varepsilon - c_1\delta < 0 \\ (2-\rho)s_k - \varepsilon + c_1\delta > 0 \end{cases}. \tag{20}$$

Therefore, we have

$$\begin{cases} s_k > -\dfrac{\varepsilon + c_1\delta}{\rho} \\ s_k > \dfrac{\varepsilon - c_1\delta}{2-\rho} \end{cases}. \tag{21}$$

Case 2: If $s_k < 0$, it obtains that

$$\begin{cases} -\rho s_k + \varepsilon + c_1\delta > 0 \\ (2-\rho)s_k + \varepsilon - c_1\delta < 0 \end{cases}. \tag{22}$$

Then, we can obtain that

$$\begin{cases} s_k < \dfrac{\varepsilon + c_1\delta}{\rho} \\ s_k < -\dfrac{\varepsilon - c_1\delta}{2-\rho} \end{cases}. \tag{23}$$

According to (12), we can obtain that

$$\varepsilon - c_1\delta > 0. \tag{24}$$

From the above, we can conclude that the sliding function of the closed-loop system with the proposed control law will converge to the QSMB region:

$$-\frac{\varepsilon - c_1\delta}{2-\rho} < s_k < \frac{\varepsilon - c_1\delta}{2-\rho}. \tag{25}$$

Thus,

$$|s_k| < \Delta = \frac{\varepsilon - c_1\delta}{2-\rho}. \tag{26}$$

This completes the proof. ■

Theorem 2. With the control law (11), the sliding mode function will first enter into QSMB within k^* steps, which is given as

$$k^* = \lfloor \log_{1-\rho} \frac{2(\varepsilon - c_1\delta)}{(2-\rho)(\rho|s_0| + \varepsilon - c_1\delta)} \rfloor + 1, \tag{27}$$

where the operator $\lfloor \cdot \rfloor$ is the nearest integer to $\cdot$, and s_0 is the initial value of the sliding function. Furthermore, s_k will never escape the QSMB after k^* steps.

Proof of Theorem 2. Firstly, we calculate the convergence step k^*.

Case 1: If $s_0 \geq 0$, according to (17), we can obtain that

$$\begin{aligned} s_1 =& (1-\rho)s_0 - \varepsilon + c_1\overline{p}_0 \\ s_2 =& (1-\rho)s_1 - \varepsilon + c_1\overline{p}_1 \\ =& (1-\rho)^2 s_0 - (1-\rho)(\varepsilon - c_1\overline{p}_0) - \varepsilon + c_1\overline{p}_0 \\ & . \\ s_k =& (1-\rho)^k s_0 - \sum_{j=0}^{k-1}(1-\rho)^{k-1-j}[\varepsilon - c_1\overline{d}_j]. \end{aligned} \tag{28}$$

Combining with the bounded $|\overline{p}_k| < \delta$, it is derived that

$$\begin{aligned} s_k \leq& (1-\rho)^k s_0 - \sum_{j=0}^{k-1}(1-\rho)^{k-1-j}[\varepsilon - c_1\delta] \\ =& (1-\rho)^k s_0 - (\varepsilon - c_1\delta)\frac{1-(1-\rho)^k}{\rho} < \frac{\varepsilon - c_1\delta}{2-\rho}. \end{aligned} \tag{29}$$

Assuming k^t is the exact time cross the QSMB, it can be derived that

$$(1-\rho)^{k^t} s_0 = (\varepsilon - c_1\delta)\frac{1-(1-\rho)^{k^t}}{\rho} + \frac{\varepsilon - c_1\delta}{2-\rho},$$

$$(1-\rho)^{k^t} = \frac{2(\varepsilon - c_1\delta)}{(2-\rho)(\rho s_0 + \varepsilon - c_1\delta)}. \tag{30}$$

Thus,

$$k^* = \lfloor k^t \rfloor + 1 = \lfloor \log_{1-\rho} \frac{2(\varepsilon - c_1\delta)}{(2-\rho)(\rho s_0 + \varepsilon - c_1\delta)} \rfloor + 1 \tag{31}$$

Case 2: If $s_0 \leq 0$, we can obtain that

$$\begin{aligned} s_k =& (1-\rho)^k s_0 + \sum_{j=0}^{k-1} (1-\rho)^{k-1-j} [\varepsilon + c_1 \overline{p}_j] \\ \geq& (1-\rho)^k s_0 + \sum_{j=0}^{k-1} (1-\rho)^{k-1-j} [\varepsilon - c_1\delta] \\ =& (1-\rho)^k s_0 + (\varepsilon - c_1\delta) \frac{1-(1-\rho)^k}{\rho}. \end{aligned} \tag{32}$$

Similarity, it is derived that

$$(1-\rho)^{k^t} s_0 + (\varepsilon - c_1\delta) \frac{1-(1-\rho)^{k^t}}{\rho} = -\frac{\varepsilon - c_1\delta}{2-\rho}. \tag{33}$$

$$(1-\rho)^{k^*}(-s_0) = (\varepsilon - c_1\delta) \frac{1-(1-\rho)^{k^*}}{\rho} + \frac{\varepsilon - c_1\delta}{2-\rho}. \tag{34}$$

Thus,

$$\begin{aligned} k^* =& \lfloor k^t \rfloor + 1 \\ =& \lfloor \log_{1-\rho} \frac{2(\varepsilon - c_1\delta)}{(2-\rho)(\rho(-s_0) + \varepsilon - c_1\delta)} \rfloor + 1. \end{aligned} \tag{35}$$

Therefore, k^* is given as (27).

Next, we will give the proof of s_k remaining in QSMB after k^* steps.

Case 1: If $s_0 > 0$, it follows that

$$0 < s_{k^*} < \frac{\varepsilon - c_1\delta}{2-\rho}. \tag{36}$$

According to (17), we can obtain that

$$\begin{aligned} s_{k^*+1} - s_{k^*} =& \rho s_{k^*} - \varepsilon + c_1 \overline{p}_k \\ <& \frac{\varepsilon - c_1\delta}{2-\rho} \rho - \varepsilon + c_1 \overline{p}_k \\ <& \frac{\varepsilon - c_1\delta}{2-\rho} \rho - \varepsilon + c_1\delta \\ =& -2(\varepsilon - c_1\delta) \frac{1-\rho}{2-\rho} < 0. \end{aligned} \tag{37}$$

Therefore, it is obtained that

$$s_{k^*+1} < \frac{\varepsilon - c_1\delta}{2-\rho}. \tag{38}$$

Case 2: If $s_0 < 0$, it follows that

$$-\frac{\varepsilon - c_1\delta}{2-\rho} < s_{k^*} < 0. \tag{39}$$

Similarly, we can deduce that

$$\begin{aligned} s_{k^*+1} - s_{k^*} =& \rho s_{k^*} + \varepsilon + c_1 \overline{p}_k \\ >& -\rho \frac{\varepsilon - c_1\delta}{2-\rho} + \varepsilon + c_1 \overline{p}_k \\ >& -\rho \frac{\varepsilon - c_1\delta}{2-\rho} + \varepsilon - c_1\delta \\ =& 2(\varepsilon - c_1\delta) \frac{1-\rho}{2-\rho} > 0. \end{aligned} \tag{40}$$

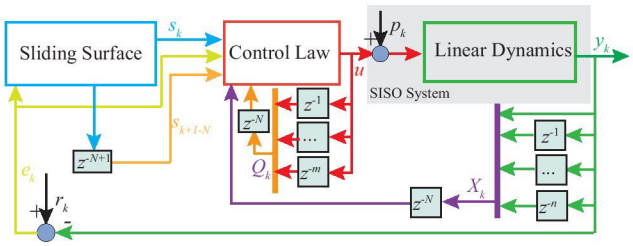

Fig. 1: Block diagram of the proposed DTITSMRC control scheme.

Therefore, it is obtained that

$$s_{k^*+1} > -\frac{\varepsilon - c_1\delta}{2-\rho}. \tag{41}$$

Therefore, $|s_{k^*+1}| < \Delta$. It can be deduced that $s_{k^*+M} < \Delta$ for any positive integer M. This completes the proof. ■

3.3 Overall Control Law

To alleviate the discontinuity of the sign function $\mathrm{sgn}(s_k)$, a boundary layer technique presented in [25] is applied, where the discontinuous function is replaced by a saturation function defined as

$$\mathrm{sat}(s_k) = \begin{cases} \mathrm{sgn}(s_k), & \text{if } |s_k| > \phi \\ \dfrac{s_k}{\phi}, & \text{if } |s_k| \leq \phi, \end{cases} \tag{42}$$

where the positive constant ϕ is the boundary layer thickness. Hence, the overall control law is given by

$$\begin{aligned} u_k =& u_{k-N} + (c_1 CB)^{-1} [(1-\rho) s_k - \varepsilon \mathrm{sat}(s_k) - c_2 E_k - \\ & c_1 CA(X_k - X_{k-N}) + c_1 CW Q_{k-N} - s_{k+1-N} + \\ & c_2 E_{k-N}]. \end{aligned} \tag{43}$$

The overall control scheme is demonstrated in Fig. 1.

4 Simulation Case

In this section, a second-order discrete-time SISO system is employed for the simulations with the state-space representation as

$$\begin{aligned} A =& \begin{bmatrix} 0 & 1 \\ -0.7423 & 1.2841 \end{bmatrix}, B = \begin{bmatrix} 0 \\ 0.9150 \end{bmatrix}, \\ C =& \begin{bmatrix} 0 & 1 \end{bmatrix}, W = \begin{bmatrix} 0 \\ 0.8270 \end{bmatrix}. \end{aligned} \tag{44}$$

The sampling rate is set as 2000 Hz. Moreover, a discrete-time sliding mode control (DTSMC) with the sliding function (7) is developed for comparisons, and the control law is given as,

$$\begin{aligned} u_k =& (c_1 CB)^{-1} [(1-\rho) s_k - \varepsilon \mathrm{sgn}(s_k) - c_2 E_k - c_1 CA X_k \\ & - c_1 CW Q_k + c_1 r_{k+1}]. \end{aligned} \tag{45}$$

The parameters in DTITSMRC are set as $c_1 = 0.007, c_2 = 1.2, \alpha = 0.99, \varepsilon = 0.01, \rho = 0.9$, and the parameters of DTSMC are same as DTITSMRC for a fair comparison.

In the first case, the sinusoidal wave with frequency 10 Hz and amplitude 5 μm without disturbance p_k is tested for

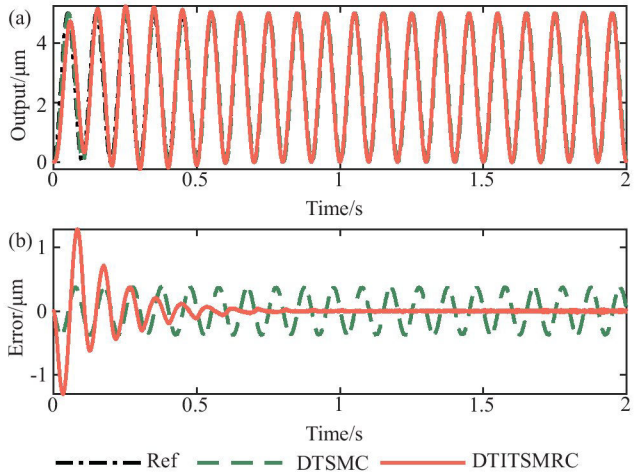

Fig. 2: Tracking results 10 Hz sinusoidal wave w/o p_k. (a) Reference signal tracking performance. (b) Tracking errors.

Table 1: Tracking Performance of Different Controllers at Steady State

Case	DTSMC(μm)		DTITSMRC(μm)	
Sinusoidal Wave w/o p_k	e_{rms}	0.2625	e_{rms}	0.0069
	e_{max}	0.3800	e_{max}	0.0199
Triangular Wave w/o p_k	e_{rms}	0.2877	e_{rms}	0.0418
	e_{max}	0.3670	e_{max}	0.0917
Sinusoidal Wave w/ p_k	e_{rms}	0.2627	e_{rms}	0.0081
	e_{max}	0.3897	e_{max}	0.0249

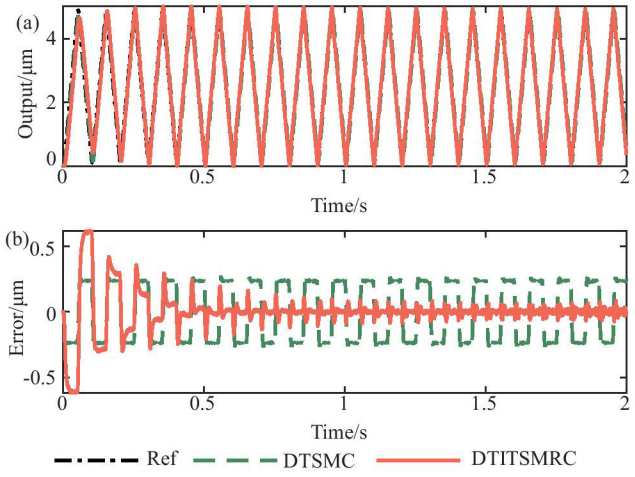

Fig. 3: Tracking results 10 Hz triangular wave w/o p_k. (a) Reference signal tracking performance. (b) Tracking errors.

DTSMC and DTITSMRC, respectively. The tracking results are plotted in Fig. 2, and the root-mean square error (e_{rms}) and maximal error (e_{max}) calculated at the steady state, i.e., the last period, are recorded in Table. 1. During the learning phase of DTITSMRC, the error is larger than that of DTSMC; while after 1s, the performance of DTITSMRC is improved significantly due to the learning of stored information. At the steady state, the e_{rms} and e_{max} are 0.0069 μm and 0.0199 μm, respectively in comparison with these of 0.2625 μm and 0.3800 μm for DTSMC.

The triangular wave with frequency 10 Hz and amplitude 5 μm without disturbance p_k is also as the periodic reference signal as shown in Fig. 3. To avoid the discontinuity at the

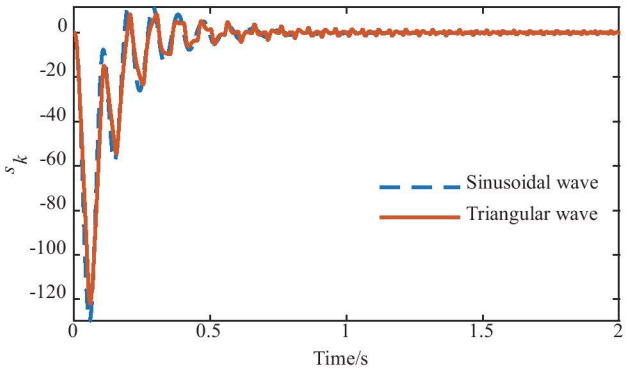

Fig. 4: Sliding function of DTITSMRC w/o p_k.

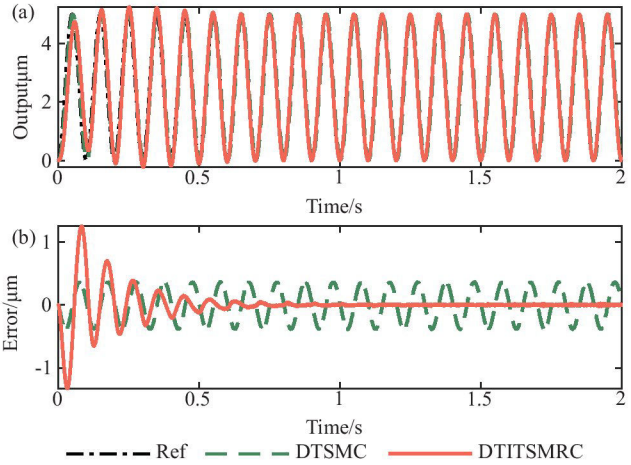

Fig. 5: Tracking results 10 Hz sinusoidal wave w/ p_k. (a) Reference signal tracking performance. (b) Tracking errors.

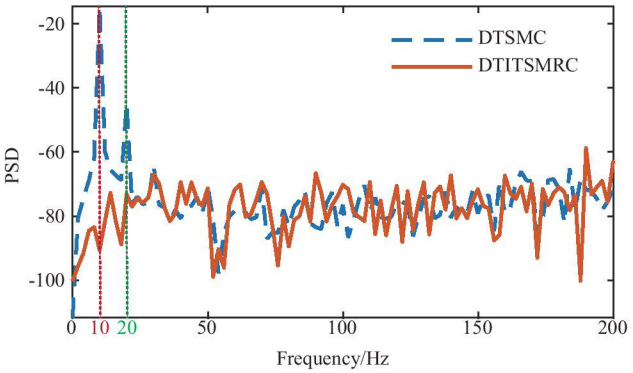

Fig. 6: Power spectral density (PSD) of errors at 10 Hz sinusoidal wave w/ p_k for different controllers.

corner, this reference is passed by a low-pass filter. Similarly to the results of sinusoidal wave, DTITSMRC achieves the best performance after several cycles' learning. The e_{rms} and e_{max} are 0.0418 μm and 0.0917 μm, respectively, which improves by 85.47% and 75.01% in contrast to DTSMC. The sliding mode function s_k of DTITSMRC for sinusoidal and triangular waves are given in Fig. 4, showing the convergence of s_k after 1s through several learning cycles.

Finally, the disturbance $p_k = 0.01\sin(2\pi \cdot 20k)$ is injected into the system to test the robustness of the controller to external disturbance. With the 10 Hz sinusoidal wave as the reference signal, the tracking results of the two controllers

are demonstrated in Fig. 5. It is clear that DTITSMRC gets the better performance at the steady state with e_{rms} of 0.0081 μm and e_{max} of 0.0249 μm. For a clear comparison, the power spectral density (PSD) of errors for the two controllers are plotted in Fig. 6. It can be observed that DTSMC generates high peaks at 10 Hz caused by the reference signal and 20 Hz caused by external disturbance, while DTITSMC could compensate these errors effectively with lower PSD at these regions.

5 Conclusions

In this paper, a control scheme called DTITSMRC is developed to achieve the precision tracking of periodic trajectories for the discrete-time SISO system. The fast convergence and robustness to unexpected disturbance are guaranteed by the integral terminal sliding function, and a learning based repetitive control is integrated into the scheme to further improve the performance through learning the information of the previous period. The constrained QSMB and finite-time steps to this band are also proven, respectively. The controller is realized only by using the measured historical output data and calculated control input without any state observer. Various simulation cases are conducted on a second-order plant. The results show that the proposed DTITSMRC presents better tracking performance for sinusoidal and triangular waves, even subjecting to external disturbance in comparison with DTSMC.

It should be noted that the method in this paper requires that the number of sample points per period N should be an integer. Thus, the fractional-order technique may be further utilized to realize the precision tracking of signals with arbitrary frequencies.

References

[1] K. Shao, J. Zheng, H. Wang, X. Wang, R. Lu, and Z. Man, "Tracking control of a linear motor positioner based on barrier function adaptive sliding mode," *IEEE Transactions on Industrial Informatics*, vol. 17, no. 11, pp. 7479–7488, 2021.

[2] J. Zheng, H. Wang, Z. Man, J. Jin, and M. Fu, "Robust motion control of a linear motor positioner using fast nonsingular terminal sliding mode," *IEEE/ASME Transactions on Mechatronics*, vol. 20, no. 4, pp. 1743–1752, 2014.

[3] Z. Feng, M. Ming, J. Ling, X. Xiao, Z.-X. Yang, and F. Wan, "Fractional delay filter based repetitive control for precision tracking: Design and application to a piezoelectric nanopositioning stage," *Mechanical Systems and Signal Processing*, vol. 164, p. 108249, 2022.

[4] M. S. Rana, H. R. Pota, and I. R. Petersen, "A survey of methods used to control piezoelectric tube scanners in high-speed afm imaging," *Asian Journal of Control*, vol. 20, no. 4, pp. 1379–1399, 2018.

[5] J. Ling, M. Rakotondrabe, Z. Feng, M. Ming, and X. Xiao, "A robust resonant controller for high-speed scanning of nanopositioners: design and implementation," *IEEE Transactions on Control Systems Technology*, vol. 28, no. 3, pp. 1116–1123, 2019.

[6] H. Komurcugil, S. Biricik, S. Bayhan, and Z. Zhang, "Sliding mode control: Overview of its applications in power converters," *IEEE Industrial Electronics Magazine*, vol. 15, no. 1, pp. 40–49, 2020.

[7] Y. Shtessel, C. Edwards, L. Fridman, A. Levant *et al.*, *Sliding mode control and observation*. Springer, 2014, vol. 10.

[8] M. Ming, W. Liang, Z. Feng, J. Ling, A. Al Mamun, and X. Xiao, "Pid-type sliding mode-based adaptive motion control of a 2-dof piezoelectric ultrasonic motor driven stage," *Mechatronics*, vol. 76, p. 102543, 2021.

[9] X. Yu, Y. Feng, and Z. Man, "Terminal sliding mode control–an overview," *IEEE Open Journal of the Industrial Electronics Society*, vol. 2, pp. 36–52, 2020.

[10] Z. Feng, W. Liang, J. Ling, X. Xiao, K. K. Tan, and T. H. Lee, "Adaptive robust impedance control for an ear surgical device with soft interaction," *IEEE/ASME Transactions on Mechatronics*, 2021, early access, doi:10.1109/TMECH.2021.3087014.

[11] V. Utkin, A. Poznyak, Y. Orlov, and A. Polyakov, "Conventional and high order sliding mode control," *Journal of the Franklin Institute*, vol. 357, no. 15, pp. 10 244–10 261, 2020.

[12] Q. Xu, "Piezoelectric nanopositioning control using second-order discrete-time terminal sliding-mode strategy," *IEEE Transactions on industrial electronics*, vol. 62, no. 12, pp. 7738–7748, 2015.

[13] H. Du, X. Yu, M. Z. Chen, and S. Li, "Chattering-free discrete-time sliding mode control," *Automatica*, vol. 68, pp. 87–91, 2016.

[14] D. A. Bristow, M. Tharayil, and A. G. Alleyne, "A survey of iterative learning control," *IEEE control systems magazine*, vol. 26, no. 3, pp. 96–114, 2006.

[15] Y. Shan and K. K. Leang, "Design and control for high-speed nanopositioning: serial-kinematic nanopositioners and repetitive control for nanofabrication," *IEEE Control Systems Magazine*, vol. 33, no. 6, pp. 86–105, 2013.

[16] A. A. Eielsen, J. T. Gravdahl, and K. K. Leang, "Low-order continuous-time robust repetitive control: Application in nanopositioning," *Mechatronics*, vol. 30, pp. 231–243, 2015.

[17] A. Sabanovic, "Variable structure systems with sliding modes in motion control—a survey," *IEEE Transactions on Industrial Informatics*, vol. 7, no. 2, pp. 212–223, 2011.

[18] H. Hou, X. Yu, L. Xu, R. Chuei, and Z. Cao, "Discrete-time terminal sliding-mode tracking control with alleviated chattering," *IEEE/ASME Transactions on Mechatronics*, vol. 24, no. 4, pp. 1808–1817, 2019.

[19] W. Gao, Y. Wang, and A. Homaifa, "Discrete-time variable structure control systems," *IEEE transactions on Industrial Electronics*, vol. 42, no. 2, pp. 117–122, 1995.

[20] H. Ma, J. Wu, and Z. Xiong, "Discrete-time sliding-mode control with improved quasi-sliding-mode domain," *IEEE Transactions on Industrial Electronics*, vol. 63, no. 10, pp. 6292–6304, 2016.

[21] H. Ma, Y. Li, and Z. Xiong, "Discrete-time sliding-mode control with enhanced power reaching law," *IEEE Transactions on Industrial Electronics*, vol. 66, no. 6, pp. 4629–4638, 2018.

[22] Z. Feng, W. Liang, J. Ling, X. Xiao, K. K. Tan, and T. H. Lee, "Integral terminal sliding-mode-based adaptive integral backstepping control for precision motion of a piezoelectric ultrasonic motor," *Mechanical Systems and Signal Processing*, vol. 144, p. 106856, 2020.

[23] M. L. Nguyen, X. Chen, and F. Yang, "Discrete-time quasi-sliding-mode control with prescribed performance function and its application to piezo-actuated positioning systems," *IEEE Transactions on Industrial Electronics*, vol. 65, no. 1, pp. 942–950, 2017.

[24] X. Yu, B. Wang, and X. Li, "Computer-controlled variable structure systems: The state-of-the-art," *IEEE Transactions on Industrial Informatics*, vol. 8, no. 2, pp. 197–205, 2011.

[25] J.-J. E. Slotine, W. Li *et al.*, *Applied nonlinear control*. Prentice hall Englewood Cliffs, NJ, 1991, vol. 199, no. 1.